ISSN: 0067-2904

Biological Activities of Silver Nanoparticles and Synergism Effects with Lincomycin Conjugation

Amna M. Abduljabar *, Nehia N. Hussein
Division of Biotechnology, Department of Applied Sciences, University of Technology, Baghdad, Iraq

Received: 7/10/2022 Accepted: 17/1/2023 Published: 30/12/2023

Abstract

Antimicrobial resistance is considered a problem for public health globally. New forms of resistance mechanisms are developing and spreading daily around the world. For that reason, a potential method for overcoming the antimicrobial resistance of several pathogens that cause deadly infections is the use of silver nanoparticles. In the present study, silver nanoparticles (AgNPs) and AgNPs conjugated with lincomycin were synthesized and characterized. The antimicrobial activity of AgNPs alone and after conjugating with lincomycin was also evaluated. Transmission electron microscopy (TEM) and scanning electron microscopy (SEM) were employed to determine the morphological properties of AgNPs and AgNPs-lincomycin, which showed the average mean size was ±26.73 nm for AgNPs and ±28.31 nm for AgNPs-lincomycin with a spherical shape. In addition, the dynamic light scattering (DLS) and zeta potential were assessed. The results showed an improvement in the antimicrobial activity of lincomycin after conjugation with AgNPs, as the inhibition zone diameter reached 45.66±1.52 mm for *Staphylococcus warneri*, 17±2 mm for *Serratia marcescens*, and 22.33±1.52 mm for *Candida guilliermondii*. It also showed a synergistic effect of AgNPs-lincomycin against the biofilm formation of *Candida guilliermondii*, whereas *Serratia marcescens* was slightly affected. The MIC of AgNPs was 25 µg/ml for *Staphylococcus warneri* and *Candida guilliermondii*, whereas 100 µg/ml for *Serratia marcescens*, when the MIC of AgNPs-lincomycin was 12.5 µg/ml for *Staphylococcus warneri* and *Candida guilliermondii*, and 100 µg/ml for *Serratia marcescens*. In the experiment of the effect of AgNPs on gene expression of the antibiotic resistance genes, including the *blaZ* gene in *Staphylococcus warneri*, the *aac(6′)-Ib-cr* gene in *Serratia marcescens*, and the *CDR1* gene in *Candida guilliermondii*, the results showed that there was a decrease in gene expression after being treated with AgNPs in each gene.

Keywords: Anti-microbial activity; Synergistic effect; Silver nanoparticles; Lincomycin; Gene expression.

الأنشطة البيولوجية لجسيمات الفضة النانوية والتأثير التآزري عند اقترانها مع الينكومايسين

أمنة منذر عبد الجبار* ,نهاية نعمة حسين

فرع التقنيات الاحيائية ، قسم العلوم التطبيقية ، الجامعة التكنولوجية ، بغداد ، العراق

*Email: as.20.30@grad.uotechnology.edu.iq

الخلاصة

تعتبر مقاومة مضادات الميكروبات مشكلة للصحة العامة على مستوى العالم. أشكال جديدة من آليات المقاومة تتطور وتنتشر يوميا في جميع أنحاء العالم. لهذا السبب ، فإن الطريقة المحتملة للتغلب على مقاومة مضادات الميكروبات للعديد من مسببات الأمراض التي تسبب العدوى المميتة هي استعمال جزيئات الفضة النانوية. في الدراسة الحالية ، تم تصنيع وتوصيف جزيئات الفضة النانوية (AgNPs) وجزيئات الفضة النانوية المقترنة مع اللنكومايسين(AgNPs– lincomycin) . كما تم تقيم النشاط المضاد للميكروبات لكل من جزيئات الفضة النانوية لوحدها وبعد اقترانها مع اللنكومايسين. تم إستعمال كل من المجهر الألكتروني النافذ (TEM) و المجهر الإلكتروني الماسح (SEM) لتحديد الخصائص المورفولوجية لـ AgNPs و AgNPs– lincomycin و التي أظهرت أن متوسط الحجم كان 26.73 ± نانوميتر لـ AgNPs و 28.31± نانومتر لـ AgNPs– lincomycin وامتلاكها الشكل الكروي. بالإضافة إلى ذلك ، تم تقييم تشتت الضوء الديناميكي (DLS) وجهد زيتا (zeta potential) . أظهرت النتائج تحسناً في النشاط المضاد للميكروبات للينكومايسين بعد اقترانه مع AgNPs حيث بلغ قطر منطقة التثبيط 1.52 ± 45.66 لبكتريا *Staphylococcus warneri* ± 2, 17ملم لبكتريا *Serratia marcescens* و 1.52 ± 22.33 ملم لفطر *Candida guilliermondii*. كما أظهر AgNPs–lincomycin تأثيرًا تآزريًا مضاداً لتكوين الأغشية الحيوية لـ *Candida guilliermondii* بينما ؛ تأثر الغشاء الحيوي لبكتريا *Serratia marcescens* بشكل طفيف. كان التركيز المثبط الأدنى (MIC) لـ AgNPs هو 25 ميكروغرام / مل لكل من بكتريا *Staphylococcus warneri* وفطر *Candida guilliermondii* , بينما كان 100 ميكروغرام / مل بالنسبة لبكتريا *Serratia marcescens*.في تجربة تأثير AgNPs على التعبير الجيني لجينات مقاومة المضادات الحيوية والتي تشمل كل من جين *blaZ* في بكتريا *Staphylococcus warneri*, جين *aac(6′)-Ib-cr* في بكتريا*Serratia marcescens* و جين *CDR1*لفطر *Candida guilliermondii* أظهرت النتائج أن هناك انخفاض في التعبير الجيني لهذه الجينات بعد المعاملة بـ AgNPs.

Introduction

Recently, the increased prevalence of antimicrobial-resistant (AMR) microorganisms poses a significant challenge to healthcare systems, resulting in higher morbidity and death rates globally. Reduced production of clinically useful antibiotics has coincided with the rise of resistant bacteria. Antimicrobial resistance refers to microorganisms that can reproduce and survive in the presence of an anti-microbial agent at a concentration sufficient to inhibit or eliminate it [1].

Various alternative strategies proposed for controlling bacterial AMR have been presented, such as antibodies, essential oils, bacteriocins, and phage treatment. These substances demonstrated antibacterial action both alone and when used in combination with antibiotics (synergistic activity) [2]. Although the use of these materials is promising, it still has drawbacks, including limited storage stability, expensive pricing, and laborious and time-consuming synthesis procedures that require highly skilled staff [3].

Researchers are trying to use different nanoparticles in the pharmaceutical and biomedical sectors as alternative anti-microbial agents to solve these problems. Various metals are used for the preparation of effective nanoparticles, for example, gold, silver, and platinum [4]. Metallic nanoparticles have various features, such as stability and activity, and their distinct surface plasmon resonance makes them good drug transporters and diagnostic treatment agents. Engineered metals have been employed to synthesize NPs by modifying their size and shape of surface; biomedical research has been conducted in the development of green-synthesized metallic NPs and their uses as anticancer, antibacterial, anti-inflammatory, and antioxidant agents [5]. One of the nanoparticles used is silver nanoparticles (AgNPs), which are now

considered a source of unique antimicrobial agents and have several advantages, such as a lower tendency to induce resistance, broad-spectrum activity, and stability [6]. Microbial membranes are affected by silver nanoparticles (AgNPs). AgNPs are active as antimicrobial agents at low concentrations (mg/L) and do not have cytotoxic effects on eukaryotic cells (including human erythrocytes). The interactions between antibiotics and silver nanoparticles are the most common in studies committed to stimulating the antibiotics and nanoparticles to interact synergistically and investigating the efficiency of antibacterial and antifungal agents that are generated by the conjugation between them and nanoparticles against different pathogens, including *S. warneri, S. marcescens*, and *C. guilliermondii* [7, 8].

The physicochemical AgNPs' features, such as the small size of particles with large surface areas, allow them to penetrate cell walls and membranes and affect intracellular molecules, which leads to microbial cell death. This has been achieved in a variety of ways, including protein synthesis, metabolic pathway blockage, interference with the production of nucleic acid (DNA), and disruptions of the cell wall [9].

Some studies found that AgNPs may impact microbial resistance to antibiotics by affecting the genes that are responsible for the antibacterial activity because the nanoparticles could induce the break of single-strand DNA and affect gene expression [10].

Lincomycin, a natural product lincosamide antibiotic derived from the actinomycete Streptomyces lincolnensis, is administered to treat penicillin-allergic individuals as well as drug-resistant bacterial infections of various types [11]. However, resistance to this antibiotic is developing. As a result, the most effective strategy to prevent growing resistance is to apply alternative antimicrobials and combine other antimicrobials with antibiotics. This research aims to study the antimicrobial activity of different concentrations of AgNPs and the synergistic effect of silver nanoparticles conjugated with lincomycin against antibiotic-resistant microbes, in addition to studying the effect of silver nanoparticles on the gene expression of antibiotic resistance genes in *S. warneri, S. marcescens*, and *C. guilliermondii*.

2. MATERIAL AND METHODS

2.1 Materials

The culture media used in this study are MacConkey agar, Mannitol salt agar, Sabouraud dextrose agar, Mueller-Hinton agar, tryptone soy broth, and nutrient broth purchased from Mast, Liverpool, England. Gram stain and phosphate buffer solution (PBS) were purchased from Sigma-Aldrich, Darmstadt, Germany. Reagents and chemicals used to synthesize AgNPs, including silver nitrate (AgNO3), tri-sodium citrate dihydrate (Na3C6H5O7), and sodium dodecyl sulfate (SDS, C12H25NaSO4), were obtained from BDH, West Yorkshire, England. Antibiotic disks were obtained from Liofilchem, Italy. Lincomycin (C18H34N2O6S) was obtained from Livealth Biopharma, MS, India. The kits were obtained from TransGen Biotech, China, and utilized in accordance with the manufacturer's specs and instructions.

2.2 Identification of Microorganisms

The microorganism's isolates were collected from medical city/ Educational laboratories. The isolates were identified morphologically, microscopically, biochemically, and finally by the Vitek-2 system. The following microbes, *S. warneri, S. marcescens*, and *C. guilliermondii*, were obtained.

2.3 Antibiotic Sensitivity assay

The antibiotic sensitivity of the microbial isolates was determined using the Kirby-Bauer disk diffusion method. These antibiotics include Amikacin (AK), Amoxicillin (AX), Amoxicillin/clavulanic acid (AMC), Cefotaxime (CTX), Lincomycin (MY), Novobiocin (N0), Rifampicin (RD), Streptomycin (S), Penicillin (P), Tetracycline (TE), Trimethoprim-sulfamethoxazole (STX), Fluconazole (FLU), Ketoconazole (KCA), and Nystatin (NY) (CLSI 2021). The microbial suspension was prepared and compared with the turbidity of standard McFarland. 20 µl of the microbial suspension was spread onto the surface of Mueller Hinton agar medium by a sterilized cotton swab, and antibiotic disks were placed at a regular distance on the agar surface. The petri dishes were incubated at 37 ºC for 24 hours [12]. To detect the synergistic effect of AgNPs with antibiotics against the isolates, each antibiotic disk was saturated with 20 µl of AgNPs before being transferred to the surface of the agar plate. Then the diameters of the inhibition zones were determined. Fold increase (%) = (b-a)/a*100 was used to calculate the fold increase area, where a and b refer to the zones of inhibition for an antibiotic alone and an antibiotic + AgNPs, respectively [13].

2.4 Preparation of lincomycin antibiotic Stock solution

A stock solution of lincomycin was prepared with a final concentration of 15 µg/ml by mixing 0.2 ml from the lincomycin vial with 1 ml of distal water.

2.5 Synthesis of AgNPs by chemical method

AgNPs were prepared by the chemical reduction method according to [14] by dissolving 0.0849 g of silver nitrate ($AgNO_3$) in 100 ml of deionized water to obtain 5 mM. 0.0103 g of Tri-sodium citrate dehydrates (TSC) ($Na_3C_6H_5O_7 \cdot 2H_2O$, Mw: 294.10 µg/ml) and 0.0144 g of sodium dodecyl sulfate (SDS) ($C_{12}H_{25}NaSO_4$, Mw: 288.38 µg/ml) were dissolved in 100 ml of deionized water and, at 80 °C, added drop by drop to the $AgNO_3$ solution for half an hour with continuous stirring. The mixture was left at 80 °C for 4 hours until the color changed to yellow, then cooled to room temperature and stored in a dark container in the refrigerator.

2.6 Preparation of conjugation of AgNPs-lincomycin conjugation

100µg/ml of AgNPs was conjugated with 15µg/ml of lincomycin by mixing 0.8ml of AgNPs with 0.2ml of lincomycin. Then the solution was homogenized by an ultrasonic device and then placed in a dark container at ambient temperature [15].

2.7 Characterization of synthesized AgNPs and AgNPs-lincomycin

To assess the function of the synthesized AgNPs, characterization is an important step. Characterization is performed by scanning electron microscopy (Zeiss, Jena, Germany), zeta potential (Brookhaven, Deklab County, GA, USA), dynamic light scattering (Brookhaven, NY, USA), and transmission electron microscopy (Zeiss, Jena, Germany).

2.8 Synergistic effects evaluation

The well diffusion method was carried out to test the antimicrobial efficacy, according to [16], by using AgNPs in different concentrations (100, 50, 25, and 12.5 µg/ml), lincomycin (15 µg/ml), and a combination of AgNPs and lincomycin.

2.9 Biofilm formation test

The tube method was used to detect biofilm formation in the used microorganisms, according to [17]. A loopful of test isolates was implanted in 5 ml of tryptone soy broth in test tubes, and then the tubes were incubated for 24 hours at 37 ºC. Biofilm formation was observed before and after treatment with AgNPs in different concentrations (100, 50, 25, and 12.5 µg/ml), lincomycin (15 µg/ml), and the AgNPs-lincomycin combination.

2.10 Measurement of the MIC and MBC

The minimum inhibitory concentration (MIC) and minimum bactericidal concentration (MBC) were determined for AgNPs, lincomycin, and AgNPs-lincomycin combination against *S. warneri*, *S. marcescens,* and *C. guilliermondii*, according to [18].

2.11 Growth Curve assay

The assay was used to identify the dynamic pattern of 100 µg/ml of AgNPs activity against the growth of *S. warneri*, *S. marcescens*, and *C. guilliermondii* according to [19] with some modification. 0.1 ml of synthesized AgNPs (100 µg/ml) and 0.1 ml of microbial suspension were added to 10 ml of nutrient broth and mixed carefully, and then 10 µl of each tube was spread on the surface of the Mueller-Hinton agar plate and incubated at 37 °C for 24 hours to reveal the growth. Viable microbial cells were counted at 0, 30, 60, and 90 minutes.

2.12 Gene expression level analysis

The expression level was examined for three antibiotic resistance genes, including *blaZ, aac (6′)-Ib-cr*, and *CDR1* for *S. warneri*, *S. marcescens*, and *C. guilliermondii*, respectively. Firstly, the total RNA of microbial cells (treated and untreated with AgNPs) was extracted using an RNA extraction kit (TransZol UpPlus RNA Kit). Subsequently, total RNA extraction from samples was used to synthesize cDNA using the EasyScript® One-Step gDNA Removal and cDNA Synthesis SuperMix kit. Then the TransStart® Top Green qPCR Super Mix (TransGen, Biotech AQ131-01 kit) was used to amplify cDNA. The gene expression level of the *blaZ* gene for *S. warneri*, the primers used are (Forward 5′-ACTTCAACACCTGCTGCTGCTTTC-3′and Reverse 5′-TGACCACTTTTATCAGCAACC-3′), *aac(6′)-Ib-cr* gene for *S. marcescens*, the primers used are (Forward 5′-ATGACTGAGCATGACCTTGC-3′ and Reverse 5′-TTAGGCATCACTGCGTGTTC-3′) and the *CDR1* gene for *C. guilliermondii*, the primers used are (Forward 5’-CTTAGTCAAACCACTGGATCG-3’ and Reverse5’-CCAAAAGTGATGAAAAGGC-3’), were estimated by real-time PCR system. Real-time PCR program as follows: 94ºC (30 s), 94ºC (5 s), 52ºC (15 s), 72ºC (20 s) for 35 cycles. Finally, "$2^{-\Delta Ct}$" was assigned to the expression, which determines the alterations in the relative fold. So the results were expressed as a fold change in the level of expression of a study gene adjusted to a housekeeping gene and relative to a calibrator, which is the study gene in control samples [20].

2.13 Statistical analyses

The data were analyzed using SPSS v.24 software and a one-way analysis of variance (ANOVA) at a 0.05 level of statistical significance. The results were reported as mean ±SE. All tests were conducted in triplicate**.**

3. RESULT AND DISCUSSION

3.1 Identification of microorganisms

3.1.1 Morphological Identification of microorganisms

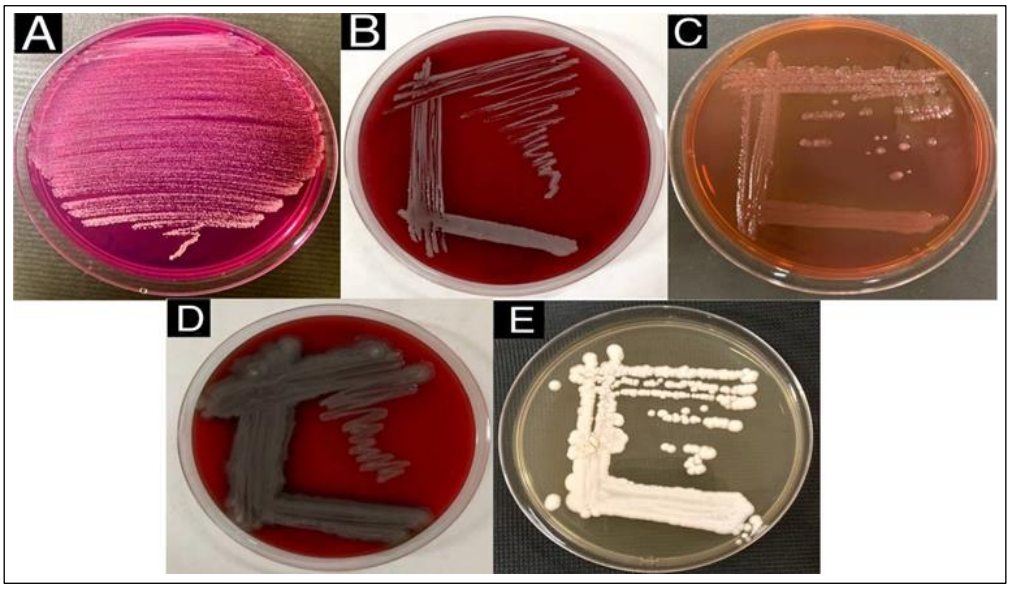

Figure 1: Morphology of: (A) *S. warneri* on Mannitol salt agar; (B) *S. warneri* on blood agar; (C) *S. marcescens* on MacConkey agar; (D) *S. marcescens* on blood agar; and (E) *C. guilliermondii* on SDA

3.2 Antimicrobial susceptibility

The disk diffusion method was used to measure the level of resistance of microbes to antibiotics and to compare it to the standard tables provided in a previous study (CLSI, 2021). The results revealed that *S. warneri* had a higher resistance rate to the three antibiotics: penicillin (P), tetracyclin (TE), and trimethoprim-sulfamethoxazole (STX), while it was sensitive to lincomycin (MY), followed by novobiocin (NO). The *S. marcescens* bacteria showed high resistance to all the antibiotics that were used in this test. These antibiotics are amikacin (AK), amoxicillin, amoxicillin/clavulanic acid (AMC), ceftazidime (CTX), lincomycin (MY), novobiocin (NO), rifampicin (RD), streptomycin (S), and tetracycline (TE). These results agree with the VITEK-2 results. *C. guilliermondii* showed high sensitivity to each ketoconazole (KCA), followed by Nystatin (NY), while it showed resistance to Fluconazole (FLU), as shown in Table 1. Then antibiotics were used in combination with AgNPs to determine the synergistic activity against the mentioned pathogens.

Table 1: Synergistic effect of different antibiotics and antibiotics with AgNPs on *S. warneri*, *S. marcescens*, and *C. guilliermondii*

Symbol	Concentration µg/disk	*S. warneri*			*S. marcescens*			*C. guilliermondii*		
		Ab*	**Ab+AgNPs***	**F.I%**	**Ab**	**Ab+AgNPs**	**F.I%**	**Ab**	**Ab+AgNPs**	**F.I%**
AK	10	-	-	-	16	18	12.5	-	-	-
AX	25	-	-	-	16	11	-31.25	-	-	-
AMC-30	20/10	-	-	-	16	10	-37.5	-	-	-
CTX	30	-	-	-	6	9	50	-	-	-
FLU	25	-	-	-	-	-	-	12	35	65,71
KCA	10	-	-	-	-	-	-	40	55	37.5
MY	15	35	45	28.57	6	13	116.7	12	22	83.33
NO	30	35	38	8.57	13	24	84.62	-	-	-
NY	100IU	-	-	-	-	-	-	32	40	25
P	10 IU	6	12	100	-	-	-	-	-	-
RD	5	-	-	-	13	13		-	-	-
S	10	-	-	-	18	22	22.22	-	-	-
TE	30	14	14		9	12	33.33	-	-	-
STX	25	6	12	100	-	-	-	-	-	-

*inhibition zone in (mm), **F.I: Fold Increase F= ((b-a)/a)*100
Note: The diameter of the disk (6 mm) was used to measure the fold increase in the absence of microbial growth inhibitory zones.

3.3 Characterization of AgNPs and AgNPs-lincomycin

The color changed gradually from colorless to dark yellow after adding the mixture of TSC and SDS, which indicated the formation of AgNPs. Dynamic light scattering (DLS) analysis results reported nonhomogeneous AgNPs with an average particle size of 35.45 nm. The presence of the three peaks in **Figure 3** indicates the polydispersity of nanoparticles (PdI = 0.336), which suggests that the nanoparticles may not be stable over a longer storage time, as well as the presence of various sizes of AgNPs in the nanoparticle solution. In the case of AgNPs-lincomycin, the result showed one peak, which indicates the dispersity of nanoparticles (PdI = 0.189) with an average particle size of 40 nm. The size obtained through DLS is often bigger than that obtained through TEM, which might be related to the effect of Brownian motion [21]. Lower PdI indicated good dispersibility, which is important for good stability. NPs due to the increased concentration after adding lincomycin, which indicated that it prevented the aggregation of NPs.

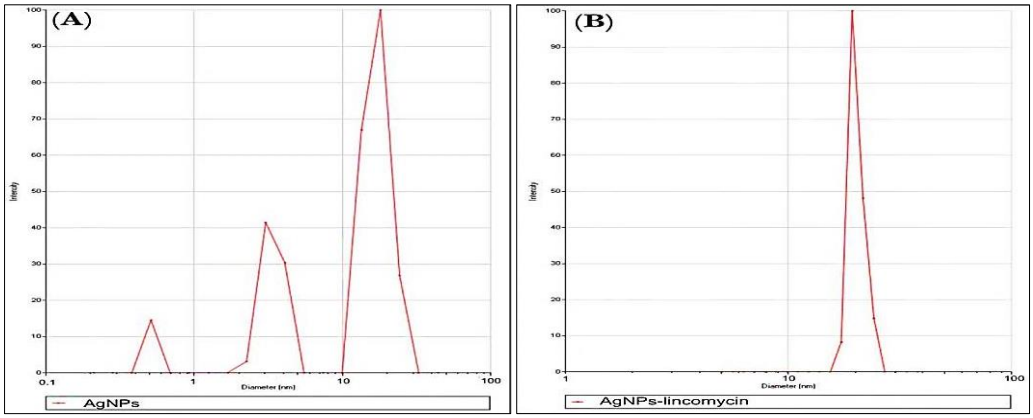

Figure 2: DLS for (A) AgNPs and (B) AgNPs-lincomycin

The TEM images in **Figure 4A** show that most of the synthesized AgNPs have small sizes and spherical forms, with an average mean size of ±26.73 nm, as also demonstrated by the histogram. The AgNPs-lincomycin in **Figure 4B** indicated that a modest increase in particle size was due to the binding and formation of AgNPs-lincomycin. The average mean size was estimated at ±28.31 nm, as also demonstrated by the histogram. (The average mean size of nanoparticles was measured using Image J software).

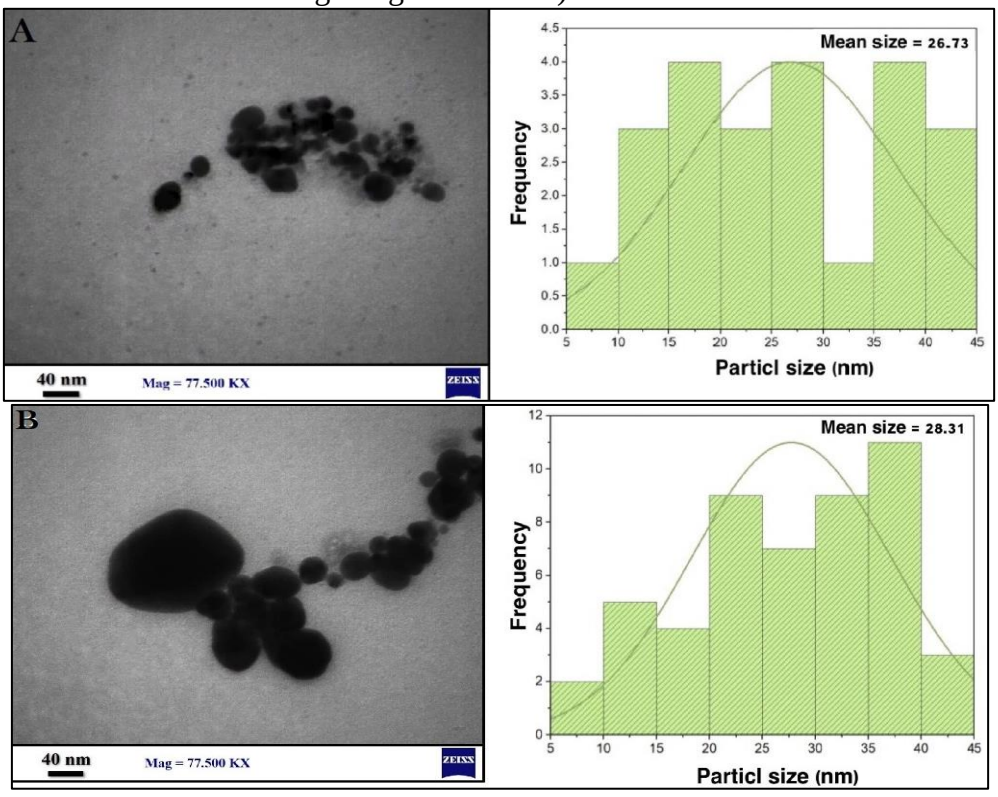

Figure 3: TEM of (A) AgNPs and (B) AgNPs-lincomycin

The SEM image of AgNPs indicated a more visible structural arrangement with a smooth surface and spherical form and particles that look equally dispersed, with a size range from 31.26 to 67.3 nm, as shown in Figure 5A. As for AgNPs-lincomycin, the SEM images shown in Figure 5B revealed various forms of NPs stuck together, which may be due to the drying of the sample before being analyzed by SEM.

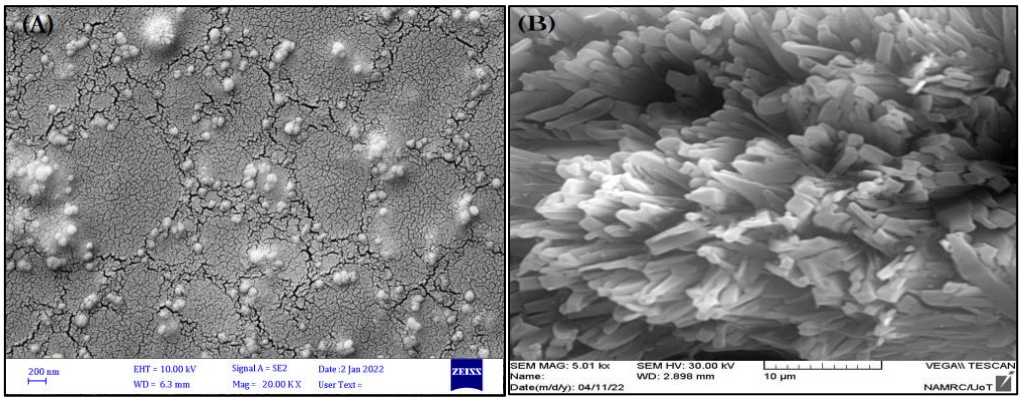

Figure 4: SEM of (A) AgNPs and (B) AgNPs lincomycin

The zeta potential analysis was employed to evaluate the AgNPs' and AgNPs-lincomycin's stability and charge on the surface. At room temperature, the zeta potential of AgNPs had negative values of 34.16 mV, indicating that AgNPs were moderately stable. As for AgNPs-lincomycin, the zeta potential at room temperature was negative (-29.89 mV), indicating moderate stability, as shown in Figure 6. Zeta potential is a key factor in influencing the stability of aqueous nanosuctions. The negative value increases particle repulsion and consequently formulation stability; negatively charged surfaces of AgNPs serve to regulate shape and size and avoid nanoparticle aggregation [22].

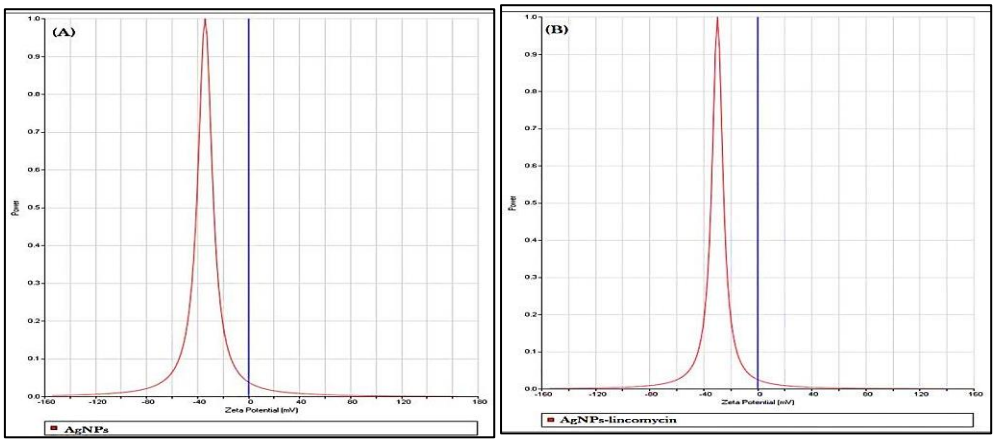

Figure 5: Zeta-potential for surface charge (A)AgNPs and (B) AgNPs-lincomycin

3.4 Synergic effect of AgNPs-lincomycin conjugation

The AgNPs were tested against *S. warneri*, *S. marcescens*, and *C. guilliermondii* at different concentrations (100, 50, 25, and 12.5) µg/ml to determine their antimicrobial activity. The inhibition zone showed that the greatest effect of AgNPs was at 100 µg/ml; it decreased with a decrease in concentration. Ag^+ inhibits the electron transport cycle in microbial cytochrome by using several antimicrobial strategies inside microbial cells. Ag^+ is in contact with the DNA and RNA of the microbial cell to cause damage, destroy the 30S ribosomal subunit, which prevents protein translation, and synthesize gram-positive bacteria in the cell wall. Additionally, Ag^+ ions produce ROS, which can be lethal to both bacterial cells and eukaryotic host cells. However, further information on environmental compatibility is necessary for the targeted usage of silver nanoparticles with antibacterial properties. The respiratory enzymes' thiol groups interact with silver nanoparticles, which may inhibit bacterial cells' respiration [23].

Lincomycin antibiotic results showed an effect on only *S. warneri* bacteria and a slight effect on *C. guilliermondii*. The mechanism of action of lincomycin on bacteria is that it acts by interfering with the metabolic pathways to prevent the synthesis of microbial proteins by binding to the 23S rRNA of the 50S subunit and imitating the intermediate formed in the initial phase of the elongation cycle [24]. On the other hand, lincomycin resistance may be produced through methylation of 23S ribosomal RNA, either by active efflux from the bacterial cell or particular enzymes altering the antibiotics [25].

The AgNPs-lincomycin combination exhibited more synergetic antimicrobial activity than lincomycin alone against microbial isolates. The formation of complexes between antibiotics and AgNPs is hypothesized as a potential mechanism demonstrating their synergistic effects. Chelation bound the antibiotic's active and functional groups, such as hydroxyl and amino groups, to the large surface area of AgNPs. However, it has been suggested that AgNPs' hydrophobic nature enhances interactions with bacterial membranes, thereby improving lincomycin transport across cell membranes [26]. The results are shown in **Figure 7, Table 2**.

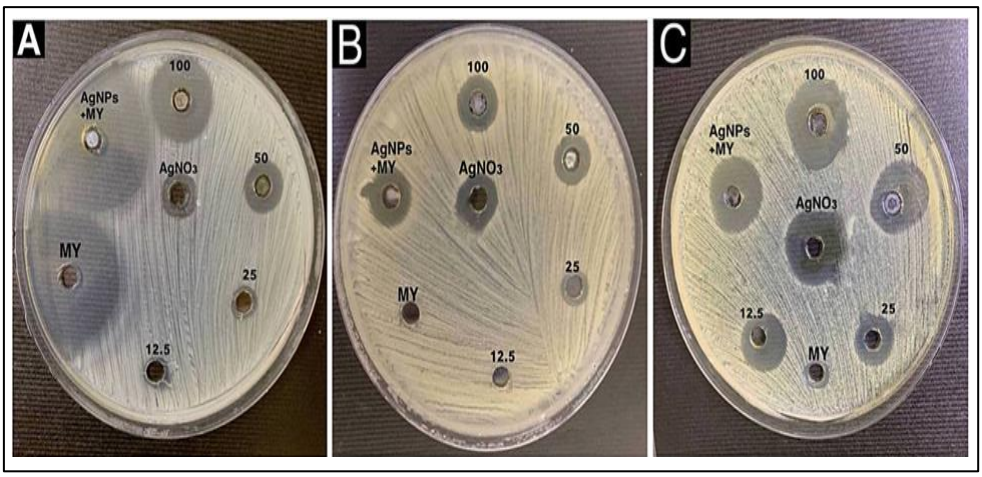

Figure 6: The inhibitory effect of different concentrations of AgNPs, AgNO3, lincomycin (MY), and AgNPs-lincomycin for (A) *S. warneri* (B) *S. marcesces* (C) *C. guilliermondii*

Table 2: Synergistic effect of lincomycin (MY) antibiotic with and without synthesized AgNPs against pathogens

Microorganisms	AgNO3	AgNPs 100µg/ml	AgNPs 50µg/ml	AgNPs 25µg/ml	AgNPs 12.5µg/ml	Lincomycin 15 µg/ml	AgNPs +lincomycin
S. warneri	18 ±2	30.33±2.51	22±2	16±1	8.66±3.05	42±2	45.66±1.52
S. marcescens	17.33±2.08	20.33±2.08	17±2.64	12.66±2.08	6±0	6±0	17±2
C. guilliermondii	25.33±1.52	34.33±0.57	30.33±1.15	24±1	19.66±0.57	12.33±0.57	22.33±1.52

3.5 Biofilm formation

The effect of various concentrations of AgNPs (100, 50, 25, and 12.5 µg/ml) on biofilm formation in these microorganisms results showed that AgNPs are capable of inhibiting biofilm production at concentrations of 100 and 50 µg/ml in *S. marcescens* while *C. guilliermondii* biofilm is inhibited at concentrations of 100, 50, and 25 µg/ml, and this is attributed to the fixation of bacteria to any surface, which is the primary stage in biofilm formation by polar flagella and the production of adhesion proteins, like type IV pili, which then enables the spread of cells to the surrounding region [27]. AgNPs fixed on the cell surface can inhibit this process. Furthermore, AgNPs facilitate the neutralization of the adhesive substances involved in the

formation of biofilm. Jena et al. reported that the AgNPs can mediate apoptosis of the bacteria cell via destroying the bacterial actin cytoskeletal network. The results show the AgNPs impact the actin cytoskeleton of MreB, leading to morphological alterations in the shape of bacteria and increased membrane fluidity, resulting in cell rupture [28]. While biofilm formation was not affected at low concentrations (12.5 µg/ml) of AgNPs in both above microorganisms, *S. warneri* bacteria did not show biofilm formation ability.

Lincomycin has no effect on biofilm formation in *S. marcescens,* and *C. guilliermondii* suggests that from the top to the bottom of biofilms, there are gradients of nutrients and oxygen. These gradients are associated with decreased bacterial metabolic activity and increased doubling times in the bacterial cells; it is these more or less dormant cells that are partly to blame for the tolerance to antibiotics [29]. The AgNPs-lincomycin combination displayed inhibition of biofilm formation in *C. guilliermondii* and a slight effect on biofilm formation in *S. marcescens*. This means that a synergistic effect occurred that led to the failure of biofilm formation in *C. guilliermondii,* as shown in **Figure 8**.

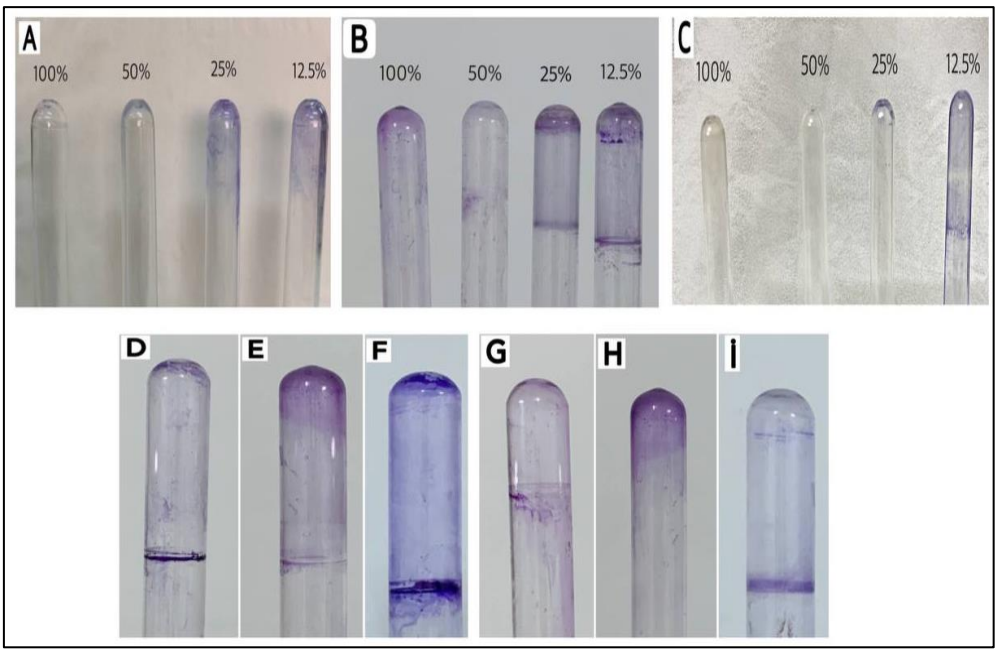

Figure 7: biofilm formation (A) AgNPs on *S. warneri,* (B) AgNPs on *S. marcescens* (c) AgNPs on *C. guilliermondii* (D) Lincomycin on *S. marcescens* (E) AgNPs-lincomycin on *S. marcescens* (F) control positive for *S. marcescens* (G) Lincomycin on *C. guilliermondii* (H) AgNPs-lincomycin on *C. guilliermondii* (I) control positive for *C. guilliermondii*

3.6 MIC and MBC determination

Each microorganism used was incubated with different concentrations of AgNPs and AgNPs-lincomycin (100, 50, 25, and 12.5 µg/ml) to detect MIC and MBC; the results are shown in Table 3. While *S. marcescens* is very resistant, no MBC appeared. Among all the microbial tests, the lowest MIC value was achieved for AgNPs-lincomycin, which demonstrated strong antimicrobial activity with a major lowering in the MIC when compared with AgNPs alone. The MBC value was influenced by some factors, such as the cell wall's composition, the bacterial synthesis of some enzymes, and bacterial suspension concentrations. Generally, the principal mechanism of action of silver nanoparticles in an aqueous microenvironment was that the AgNPs released silver ions continuously; these silver nanoparticles produced reactive oxygen species (ROS) and free radicals, which destroyed the cell wall of the microbes and stopped the respiratory enzymes [30].

Table 3: Minimum Inhibitory Concentration and Minimum Bactericidal Concentrations for a Bacterial Isolate

Microorganism	Conc. of AgNPs(µg/ml)		Conc. of AgNPs -lincomycin (µg/ml)	
	MIC	**MBC**	**MIC**	**MBC**
S. warneri	25	50	12.5	25
S. marcescens	100	-	100	-
C. guilliermondii	25	50	12.5	100

3.7 Growth curve

The growth curve assay for 100 µg/ml AgNPs was used to estimate their antimicrobial activity in the used microorganisms. The results showed that AgNPs (100 µg/ml) required 90 minutes to start killing *S. warneri* and more than 90 minutes to kill *S. marcescens*, while *C. guilliermondii* required less time to start killing at 60 minutes, as shown in **Figure 9**. AgNPs' ability to disrupt cells has not yet been fully understood. The size of AgNPs determines their ability to bind to the cell wall and the cell membrane, which is thought to result in structural alterations that induce cell death. It also proposes that AgNPs produce free radicals that destroy the cell membrane when they are in contact with cells and later cause cell death. The production of bactericidal reactive oxygen species by AgNPs, inactivation of enzymes like lactate dehydrogenase, interaction with DNA's phosphate groups, and effects on DNA replication were all discovered [31].

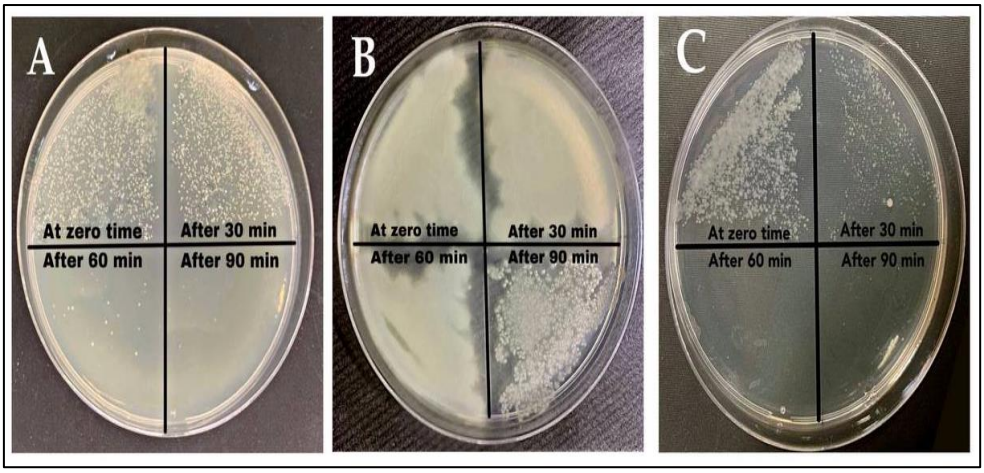

Figure 8: Growth curve assay of AgNPs against (A) *S. warneri*, (B) *S. marcescens, and* (C) *C. guilliermondii*

3.8 Gene expression analysis

3.8.1 Extraction of total RNA and Cdna Reverse Transcription

The concentration and purity of RNA were measured after isolation, and they ranged between 40 and 80 ng/µl and 1.8 and 2 ng/µl, respectively, demonstrating the excellent purity of all RNA samples. The efficiency of cDNA concentration was then evaluated using qPCR. All stages were linked with perfect yield, indicating effective reverse transcription.

3.8.2 Real-time PCR quantification of *blaZ, aac(6′)-Ib-cr* and *CDR1* gene expression

The expression level of antibiotic resistance-related genes was evaluated, and it was found that *aac(6′)-Ib-cr* and *CDR1* genes showed down-regulation in the expression level after exposure to AgNPs by 0.3487 and 0.0004 folds, respectively, as compared with the untreated

control group. While blaZ gen revealed that gene expression was slightly lesser in contrast to the control group with 0.986 fold, AgNPs may impact antibiotic resistance in microbial cultures via the antimicrobial activity of the genes because NPs can alter DNA single-strand breaks and gene expression, resulting in impaired gene expression because NPs affect the activity and sequence of promoters. This process is triggered by elevated intracellular ROS and chromosomal and oxidative DNA damage [32]. AgNPs release Ag ions within the microbial cell, which suppress replication of the DNA due to a reaction with phosphate groups in the polyanionic backbone of nucleic acids. Additionally to the interactions between metal ions' van der Walls and hydrophobic forces, as well as the oxygen and nitrogen atoms contained in nucleic acids, RNA is unlike DNA, which is more affected by oxidative damage and reactive oxygen species (ROS) production by AgNPs, and without the mechanisms of RNA repair, fundamental processes such as the regulation of transcriptional activity may be changed [33, 34]. The results are shown in **Figure 10** and **Tables 4, 5,** and **6**.

Table 4: Comparison of *blaZ* gene fold expression between groups in this study

Groups	Mean Ct of *blaZ*	Mean Ct of HKG	ΔCt (Mean Ct of *blaZ*- Mean Ct of HKG)	$2^{-\Delta Ct}$	experimental group/ Control group	Fold of gene expression
Group 1 (control)	30.000	24.200	5.800	0.0179	0.0179/0.0179	1.000
Group 2 (After AgNPs treatment)	30.000	24.180	5.820	0.0177	0.0177/0.0179	0.986

Table 5: Comparison of *aac(6′)-Ib-cr* gene Fold expression between groups in this study

Groups	Mean Ct of *aac(6′)-Ib-cr*	Mean Ct of HKG	ΔCt (Mean Ct of *aac(6′)-Ib-cr* - Mean Ct of HKG)	$2^{-\Delta Ct}$	experimental group/ Control group	Fold of gene expression
Group 1 (control)	20.88	24.7	-3.8200	14.12	14.12/14.12	1.0000
Group 2 (After AgNPs treatment)	22.51	24.81	-2.3000	4.92	4.92/14.12	0.3487

Table 6: Comparison of *CDR1* gene fold expression between groups in this study

Groups	Mean Ct of *CDR1*	Mean Ct of HKG	ΔCt (Mean Ct of *CDR1*- Mean Ct of HKG)	$2^{-\Delta Ct}$	experimental group/ Control group	Fold of gene expression
Group 1 (control)	30.64	21.46	9.1800	0.00172	0.00172/0.00172	1.0000
Group 2 (After AgNPs treatment)	42.0	21.44	20.5600	0.000001	0.000001/0.00172	0.0004

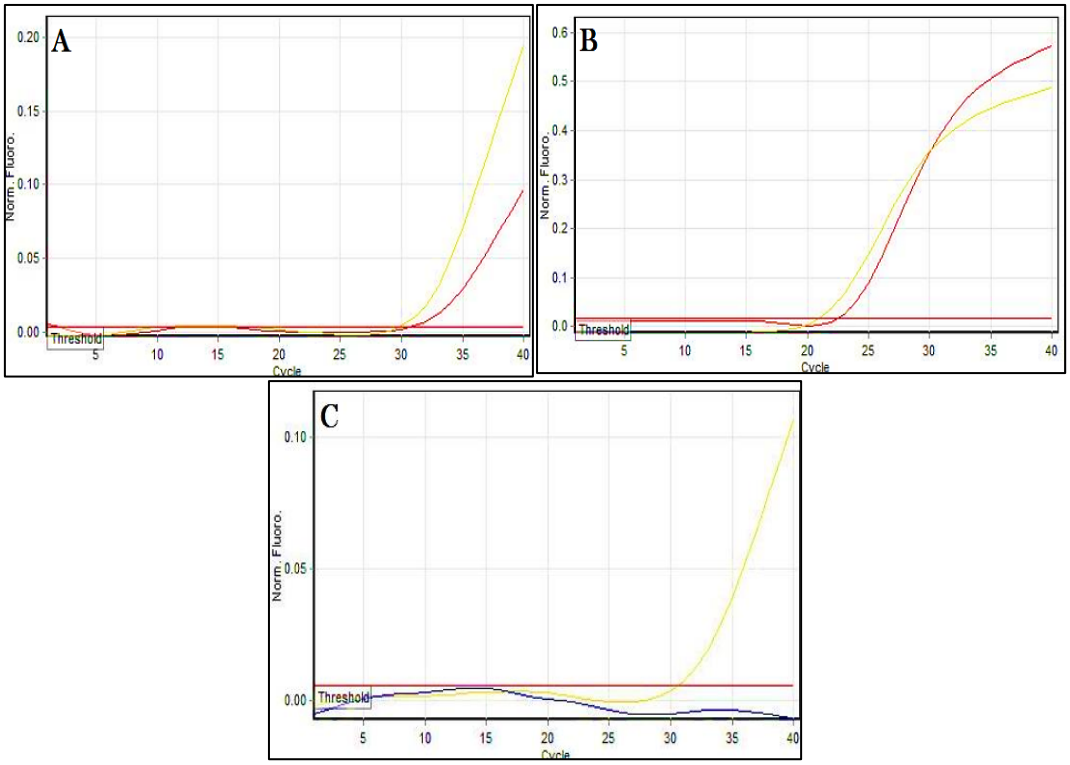

Figure 9: (A) *blaZ* gene (B) *aac(6′)-Ib-cr* gene (C) *CDR1* gene amplification plots by qPCR samples before and after treatment with AgNPs. The image was taken directly from the Cepheid (smart cycler) qPCR machine**.**

4. Conclusion

The present study found that the combination of the lincomycin antibiotic with chemically prepared AgNPs provided an effective antimicrobial against pathogenic isolates, i.e., *S. warneri*, *S. marcescens*, and *C. guilliermondii*, particularly in comparison to the Ag nanoparticles and lincomycin alone. This contributed to overcoming these microbes' pharmacological resistance to lincomycin. The chemical reduction approach employed to synthesize the AgNPs produced stable nanoparticles, and the physical and chemical properties of the AgNPs and AgNPs-lincomycin were evaluated in the analysis of shape, size, stability, and surface charge. After being exposed to AgNPs, gene expression levels of selected genes in *S. warneri*, *S. marcescens*, and *C. guilliermondii* suggest that microbial cells responded quickly to the harsh circumstances induced by AgNPs. Additionally, AgNPs have the potential to be genotoxic, damaging DNA and RNA as well as preventing cell replication and expression of genetic information, accompanied by a mutagenic effect. This kind of activity may be attributed to both the direct effects of NPs and metal ion formation as well as the indirect effects via Save Our Soul (SOS) reactions in bacterial cells that are mediated and initiated by reactive oxygen species (ROS). These results confirmed these nanoparticles' promising potential and provide compelling evidence for developing this material as an effective therapeutic alternative for treating various infections.

Conflict of Interest

References

[1] A. M. Alotaibi et al., "Silver Nanoparticle-Based Combinations with Antimicrobial Agents against Antimicrobial-Resistant Clinical Isolates," *Antibiotics*, vol. 11, no. 9, p. 1219, Sep. 2022.

[2] E. Nefedova, N. Shkil, R. Luna Vazquez-Gomez, D. Garibo, A. Pestryakov, and N. Bogdanchikova, "AgNPs Targeting the Drug Resistance Problem of Staphylococcus aureus:

Susceptibility to Antibiotics and Efflux Effect," *Pharmaceutics*, vol. 14, no. 4, p. 763, Mar. 2022.

[3] R. Vivas, A. A. T. Barbosa, S. S. Dolabela, and S. Jain, "Multidrug-Resistant Bacteria and Alternative Methods to Control Them: An Overview," *Microbial Drug Resistance*, vol. 25, no. 6, pp. 890–908, Jul. 2019.

[4] S. R. Kabir et al., "Zizyphus mauritiana Fruit Extract-Mediated Synthesized Silver/Silver Chloride Nanoparticles Retain Antimicrobial Activity and Induce Apoptosis in MCF-7 Cells through the Fas Pathway," *ACS Omega*, vol. 5, no. 32, pp. 20599–20608, Aug. 2020.

[5] S. N. Hawar, H. S. Al-Shmgani, Z. A. Al-Kubaisi, G. M. Sulaiman, Y. H. Dewir, and J. J. Rikisahedew, "Green Synthesis of Silver Nanoparticles from Alhagi graecorum Leaf Extract and Evaluation of Their Cytotoxicity and Antifungal Activity," *Journal of Nanomaterials*, vol. 2022, pp. 1–8, Jan. 2022.

[6] M. Rai, K. Kon, A. Ingle, N. Duran, S. Galdiero, and M. Galdiero, "Broad-spectrum bioactivities of silver nanoparticles: the emerging trends and future prospects," *Applied Microbiology and Biotechnology*, vol. 98, no. 5, pp. 1951–1961, Jan. 2014.

[7] U. H. Abo-Shama et al., "Synergistic and Antagonistic Effects of Metal Nanoparticles in Combination with Antibiotics Against Some Reference Strains of Pathogenic Microorganisms" *Infection and Drug Resistance*, vol. 13, pp. 351–362, Feb. 2020.

[8] S. Krajewski et al., "Hemocompatibility evaluation of different silver nanoparticle concentrations employing a modified Chandler-loop in vitro assay on human blood," *Acta Biomaterialia*, vol. 9, no. 7, pp. 7460–7468, Jul. 2013.

[9] D. S. Kharitonov et al., "Anodic Electrodeposition of Chitosan–AgNP Composites Using In Situ Coordination with Copper Ions," *Materials*, vol. 14, no. 11, p. 2754, May 2021.

[10] V. Alizadeh, B. Golestani Eimani, and F. Amjady, "Genomic Effect of Silver Nanoparticles in Staphylococcus aureus Bacteria," *J Water Environ Nanotechnol*, vol. 3, no. 1, Jan. 2018.

[11] National Center for Biotechnology Information. PubChem Compound Summary for CID 3000540, Lincomycin. 2022. Available online https://pubchem.ncbi.nlm.nih.gov/compound/Lincomycin (accessed on 22 November 2022).

[12] Z. A. Khan, M. F. Siddiqui, and S. Park, "Current and Emerging Methods of Antibiotic Susceptibility Testing," *Diagnostics*, vol. 9, no. 2, p. 49, May 2019.

[13] F. Abdel-Wahab, N. El Menofy, A. El- Batal, F. Mosallam, and A. Abdulall, "Enhanced antimicrobial activity of the combination of silver nanoparticles and different β Lactam antibiotics against methicillin resistant Staphylococcus aureus isolates," *Azhar International Journal of Pharmaceutical and Medical Sciences*, vol. 1, no. 1, pp. 24–33, Jan. 2021.

[14] I. Pinzaru et al., "Stable PEG-coated silver nanoparticles – A comprehensive toxicological profile," *Food and Chemical Toxicology*, vol. 111, pp. 546–556, Jan. 2018.

[15] D. Dehghan, M. Fasihi-Ramandi, and R. Taheri, "Investigation of Synergism of Silver Nanoparticle and Erythromycin Inhibition and Detection of Exotoxin-A Gene in Pseudomonas aeruginosa Isolated from Burn Wounds Secretion," *Iranian Journal of Medical Microbiology*, vol. 14, no. 4, pp. 379–387, Jul. 2020.

[16] M. A. Kareem, R. M. Al-Bahrani, and J. A. Ghafil, "Evaluation of inhibition activity of silver nanoparticles activity against pathogenic bacteria", *Iraqi Journal of Science*, vol. 57, no. 3C, pp. 2203–2207, Feb. 2022.

[17] F. M. Abdulsada, N. N. Hussein, G. M. Sulaiman, A. Al Ali, and M. Alhujaily, "Evaluation of the Antibacterial Properties of Iron Oxide, Polyethylene Glycol, and Gentamicin Conjugated Nanoparticles against Some Multidrug-Resistant Bacteria," *Journal of Functional Biomaterials*, vol. 13, no. 3, p. 138, Sep. 2022.

[18] D. R. Ibraheem, N. N. Hussein, G. M. Sulaiman, H. A. Mohammed, R. A. Khan, and O. Al Rugaie, "Ciprofloxacin-Loaded Silver Nanoparticles as Potent Nano-Antibiotics against Resistant Pathogenic Bacteria," *Nanomaterials*, vol. 12, no. 16, p. 2808, Aug. 2022.

[19] A. Chahardehi, D. Ibrahim, S. Sulaiman, and L. Mousavi, "Time-kill Study of Ethyl Acetate Extract of Stinging Nettle on Bacillus subtilis subsp. spizizenii ATCC CRM-6633 Strain NRS 231," *Annual Research & Review in Biology*, vol. 6, no. 1, pp. 33–40, Jan. 2015.

[20] L. S. Mohammed and M. T. Flayyih, "Study the Expression of msrA, msrB and linA/linA' genes in Presence of Some Antibiotics in Methicillin Resistance Staphylococcus aureus", *Iraqi Journal of Science*, vol. 59, no. 4A, pp. 1811–1825, Oct. 2018.

[21] X.-F. Zhang, Z.-G. Liu, W. Shen, and S. Gurunathan, "Silver Nanoparticles: Synthesis, Characterization, Properties, Applications, and Therapeutic Approaches," *International Journal of Molecular Sciences*, vol. 17, no. 9, p. 1534, Sep. 2016.

[22] S. Paosen, J. Saising, A. Wira Septama, and S. Piyawan Voravuthikunchai, "Green synthesis of silver nanoparticles using plants from Myrtaceae family and characterization of their antibacterial activity," *Materials Letters*, vol. 209, pp. 201–206, Dec. 2017.

[23] Y. Khane et al., "Green Synthesis of Silver Nanoparticles Using Aqueous Citrus limon Zest Extract: Characterization and Evaluation of Their Antioxidant and Antimicrobial Properties," *Nanomaterials*, vol. 12, no. 12, p. 2013, Jun. 2022.

[24] M. Morar, K. Bhullar, D. W. Hughes, M. Junop, and G. D. Wright, "Structure and Mechanism of the Lincosamide Antibiotic Adenylyl transferase LinB," *Structure*, vol. 17, no. 12, pp. 1649–1659, Dec. 2009.

[25] T. Rezanka, J. Spizek, and K. Sigler, "Medicinal Use of Lincosamides and Microbial Resistance to Them," *Anti-Infective Agents in Medicinal Chemistry*, vol. 6, no. 2, pp. 133–144, Apr. 2007.

[26] Y. E. Abdelmawgoud, W. Abd El- Latif, N. K. Fawzy, and S. M. Elnagdy, "Prevalence of Inducible Clindamycin Resistance and Nanotechnological Control of Staphylococcus aureus Clinical Isolates," *Egyptian Journal of Botany*, vol. 62, no. 1, pp. 73–84, Jun. 2021.

[27] E. K. Saeki et al., "Effect of Biogenic Silver Nanoparticles on the Quorum-Sensing System of Pseudomonas aeruginosa PAO1 and PA14," *Microorganisms*, vol. 10, no. 9, p. 1755, Aug. 2022.

[28] E. O. Mikhailova, "Silver Nanoparticles: Mechanism of Action and Probable Bio-Application," *Journal of Functional Biomaterials*, vol. 11, no. 4, p. 84, Nov. 2020.

[29] N. Høiby, T. Bjarnsholt, M. Givskov, S. Molin, and O. Ciofu, "Antibiotic resistance of bacterial biofilms," *International Journal of Antimicrobial Agents*, vol. 35, no. 4, pp. 322–332, Apr. 2010.

[30] M. C. G. de Allori, M. Á. Jure, C. Romero, and M. E. C. de Castillo, "Antimicrobial Resistance and Production of Biofilms in Clinical Isolates of Coagulase-Negative Staphylococcus Strains," *Biological and Pharmaceutical Bulletin*, vol. 29, no. 8, pp. 1592–1596, 2006.

[31] K. Maruthai, K. Vallayyachari, T. Ravibalan, S. A. Philip, A. V. Samrot, and M. Muthuraj, "Antibacterial Activity of the Silver Nanoparticles against Escherichia coli and Enterobacter sp," *Progress in Bioscience and Bioengineering*, vol. 1, no. 1, Sep. 2017.

[32] Y. Su et al., "Metallic nanoparticles induced antibiotic resistance genes attenuation of leachate culturable microbiota: The combined roles of growth inhibition, ion dissolution and oxidative stress," *Environment International*, vol. 128, pp. 407–416, Jul. 2019.

[33] O. Metryka, D. Wasilkowski, and A. Mrozik, "Evaluation of the Effects of Ag, Cu, ZnO and TiO2 Nanoparticles on the Expression Level of Oxidative Stress-Related Genes and the Activity of Antioxidant Enzymes in Escherichia coli, Bacillus cereus and Staphylococcus epidermidis," *International Journal of Molecular Sciences*, vol. 23, no. 9, p. 4966, Apr. 2022.

[34] G. M. Saleh and S. S. Najim, "Antibacterial Activity of Silver Nanoparticles Synthesized from Plant Latex," *Iraqi Journal of Science*, vol. 61, no. 7, pp. 1579–1588, Jul. 2020.